Computational Materials Science 45 (2009) 837–844

Contents lists available at ScienceDirect

Computational Materials Science

journal homepage: www.elsevier.com/locate/commatsci

Numerical modeling of diffusion induced phase transformations in mechanically stressed lead-free alloys

Thomas Böhme [a,*,1], Wolfgang H. Müller [b], Kerstin Weinberg [c]

[a] ThyssenKrupp Steel AG, Werkstoffkompetenzzentrum Abteilung Physikalische Technik, Kaiser-Wilhelm-Straße 100, 47166 Duisburg, Germany
[b] Institut für Mechanik, Lehrstuhl für Kontinuumsmechanik und Materialtheorie (LKM), Sekr. MS-2, Technische Universität Berlin, Einsteinufer 5, 10587 Berlin, Germany
[c] Institut für Mechanik und Regelungstechnik, Lehrstuhl für Festkörpermechanik, Universität Siegen, Paul-Bonatz-Straße 9-11, 57068 Siegen, Germany

ARTICLE INFO

Article history:
Received 23 November 2007
Received in revised form 29 July 2008
Accepted 21 August 2008
Available online 2 October 2008

PACS:
64.75.Ef
66.30.–h
81.30.–t
64.70.K–
81.30.–t
62.20.F–
05.70.–a
65.40.gd

Keywords:
Solid mixtures
Diffusion
Microstructure
Phases transformation
Spinodal decomposition
Elastic stresses

ABSTRACT

The present work investigates diffusion-induced phase evolution in solid mixtures under the presence of thermo-elastic strains. Based on five statements for an entropy principle we explain how to construct the constitutive equations for the entropy flux, the stress tensor, and the diffusion flux in multi-component solid mixtures. We show, first, that the obtained results agree with the classical results of thermodynamics of fluid mixtures and, second, that they allow for a theoretical description of phase formation and evolution. Finally we specialize to binary alloys and present various numerical studies for the brazing alloy Ag–Cu, for which the required material data is reliably documented.

1. Introduction

Diffusion processes in multi-phase and multi-component solid mixtures and the accompanying micromorphological evolution represent an important field in applied as well as in theoretical materials science. For example, (lead-free) solder alloys that are typically used in microelectronic packaging show a variation of diffusion-induced "microstructures," which has a crucial influence on the strength and lifetime of the solder joint [1]. Moreover, experimental observations show that surface tensions along the phase boundaries and the presence of additional mechanical loading significantly effect the diffusion process. Based on a systematic exploitation of the Second Law of Thermodynamics (2nd law) by means of the method of LAGRANGE multipliers, Dreyer and Müller recently derived an Extended Diffusion Equation (EDE) for binary mixtures [5]. However, recent investigations show that this method of exploitation cannot generally be applied to all classes of materials (*cf.*, explanations in Section 2.2).

For this reason we revisit in Section 2.2 an entropy principle based on "well-accepted" thermodynamical concepts. In Section 3 these concepts are applied in terms of five statements to single-phase systems in order to illustrate the agreement of the obtained results with those of classical thermodynamics of fluids. Based on the incorporation of so-called Higher Gradients (HG) we proceed in Section 4 to multiphase mixtures and derive all constitutive equations required for the description of phase separation and OSTWALD ripening. Finally we specialize to binary alloys and present various numerical studies subjected to spinodal decomposition and coarsening in Ag–Cu for one and two dimensions.

* Corresponding author. Tel.: +49 (0)203 52 25882; fax: +49 (0)203 52 24123.
E-mail addresses: thomas.boehme@thyssenkrupp.com (T. Böhme), wolfgang.h.-mueller@tu-berlin.de (W.H. Müller), weinberg@imr.mb.uni-siegen.de (K. Weinberg).
[1] Former member of the Institute Für Mechanik, Tu Berlin.

0927-0256/$ - see front matter © 2008 Elsevier B.V. All rights reserved.
doi:10.1016/j.commatsci.2008.08.015

2. Elements of continuum thermodynamics

2.1. Kinematics and balance equations

In order to describe motion and deformation of a solid continuum we identify material points at time $t = t_0$ by their *reference* position vector X^i and at times $t > t_0$ by the *current* position vector $x^i = \chi^i(x^j, t)$, from which the *displacements* $u^i = x^i - X^i$ can be determined. Further quantities are the *velocity* $v^i = \mathrm{d}x^i/\mathrm{d}t$, the *deformation gradient* $F^{ij} = \mathrm{d}x^i/\mathrm{d}X^j$, and the *Jacobian* $J = \det F^{ij} \geqslant 0$. Strains within the material are characterized by the *displacement gradient* $H^{ij} = \partial u^i/\partial X^j$ or the right CAUCHY-GREEN *tensor* $C^{ij} = F^{mi}F^{mj} = J^{2/3}c^{ij}$, where $J^{2/3}$ stands for pure volumetric changes and c^{ij} (with $\det c^{ij} = 1$) for pure changes of the shape. Further strain measures are the *linearized strains* $\varepsilon^{ij} = \frac{1}{2}(H^{ij} + H^{ji})$ and GREEN's *deformation tensor* $G^{ij} = \frac{1}{2}(C^{ij} - \delta^{ij})$.

In order to describe mixtures that consist of v components $v + 4$ *primary variables* are required, namely the partial mass or particle density, ρ_α or n_α, ($\alpha = \{1, \ldots, v\}$), the barycentric velocity or the displacements, v^i or u^i, and the internal energy density, ρe. For their determination local balances hold (here without production terms and external forces), viz.

$$\frac{\partial \rho_\alpha}{\partial t} = -\frac{\partial(\rho_\alpha v^i_\alpha)}{\partial x^i} = -\frac{\partial(\rho_\alpha v^i + J^i_\alpha)}{\partial x^i} \quad \text{or} \tag{1}$$

$$\frac{\partial n_\alpha}{\partial t} = -\frac{\partial(n_\alpha v^i_\alpha)}{\partial x^i} = -\frac{\partial(n_\alpha v^i + j^i_\alpha)}{\partial x^i}, \tag{2}$$

$$\frac{\partial \rho v^i}{\partial t} = -\frac{\partial}{\partial x^j}(\rho v^j v^i - \sigma^{ij}), \tag{3}$$

$$\frac{\partial \rho \epsilon}{\partial t} = -\frac{\partial}{\partial x^j}(\rho \epsilon v^j + q^j) + \sigma^{ij}\frac{\partial v^i}{\partial x^j} \tag{4}$$

with the diffusion flux $J^i_\alpha = \rho_\alpha(v^i_\alpha - v^i)$ and $j^i_\alpha = n_\alpha(v^i_\alpha - v^i)$. We emphasize that Eq. (2) can be used alternatively to Eq. (1) in order to account for (mass–less) vacancies. As a consequence of these balances the *total particle balance* $\partial_t n + \nabla^i(nv^i) = 0$, the *total mass balance* $\partial_t \rho + \nabla^i(\rho v^i) = 0$ and its integrated form $J = \rho_0/\rho$ will hold. In this context the following relations apply ($\rho_\alpha = m_\alpha n_\alpha$):

$$\rho = \sum_\alpha \rho_\alpha \;\Rightarrow\; \sum_\alpha J^i_\alpha = \sum_\alpha m_\alpha j^i_\alpha = 0. \tag{5}$$

In order to solve the system of Eqs. (1),(3),(4) or (2)–(4) constitutive relations for the diffusion fluxes, the CAUCHY stresses σ^{ij} and the heat flux q^i are required, which link these quantities to the primary variables in a material-dependent manner.

2.2. Entropy

A key issue of thermodynamics is the question regarding a local version of the 2nd law, which leads to the question which form of the entropy flux ϕ^i shall be used. Liu [9], presented an approach from which a constitutive relation for the entropy flux results. However, recent investigations show that ϕ^i is not unique for complex materials, and this fact is not easy to reveal within Liu's procedure [6]. Therefore we formulate *five well-established statements*, which allow to perform a general exploitation of the 2nd law, also for complex materials.

1. There exist two constitutive quantities, the *entropy density* $\rho\eta$ and the *entropy flux* ϕ^i. Moreover the constitutive relation for $\rho\eta$ has the form:

$$\rho\eta = \mathscr{S}(\text{primary variables},\ \text{functions/ deri-vatives of the primary variables}). \tag{6}$$

Table 1
Arbitrary terms, following from the different balances

n_α, v^i, $\nabla^i v^i$, $\nabla^i n_\alpha$, $\nabla^i j^i_\alpha$, τ^n_α	Partial particle balance
ρ_α, v^i, $\nabla^i v^i$, $\nabla^i \rho_\alpha$, $\nabla^i J^i_\alpha$, τ^ρ_α	Partial mass balance
ρv^i, $\nabla^{\langle i} v^{j\rangle}$, $\nabla^j \sigma^{ij}$	Momentum balance
ρe, $\nabla^i(\rho e)$, $\nabla^i q^i$, σ^{ij}	Internal energy balance

2. The *local entropy balance* reads:

$$\frac{\partial \rho\eta}{\partial t} + \frac{\partial}{\partial x^i}(\rho\eta v^i + \phi^i) = \zeta. \tag{7}$$

3. The *stresses* can be decomposed into an elastic and dissipative part: $\sigma^{ij} = \sigma^{ij}_{\text{el}} + \sigma^{ij}_{\text{diss}}$.
4. The *entropy production* ζ is positive definite and of the form (flux $\times$ driving force, *i.e,* $F_z \times D_z$):

$$\zeta = \sum_z F_z D_z, \quad \zeta \geqslant 0 \quad (\text{2nd law}) \tag{8}$$

with $F_z = \{j^i_\alpha, q^i, \sigma^{ij}_{\text{diss}}\}$ and $\zeta|_{\text{eq.}} = F^{\text{eq.}}_z = 0$.
5. The *absolute temperature* is defined by $1/T = \partial\rho\eta/\partial(\rho e)$.

The balances can be interpreted as a system of algebraic equations, of which the right hand sides can be chosen arbitrarily in order to calculate the left hand sides. Using the product rule the arbitrary terms are given in Table 1 ($\nabla^{\langle i} v^{j\rangle} = \partial v^{\langle j}/\partial x^{i\rangle}$ denotes the trace-free part of $\nabla^i v^j$). Thus the constitutive equations must be constructed such that the 2nd law *is satisfied* for *any solution* of the balances (*i.e.*, for arbitrary choice of the terms in Table 1).

3. Single phase mixtures

3.1. Entropy production

In order to investigate a single phase within a v-component solid mixture the wanted primary variables are $n_1 \ldots n_v$, u^i, and ρe. According to Statement 1 in Section 2.2 we choose the following four functional representations for $\rho\eta$ (y_β: particle concentration and $\alpha = \{1, \ldots, v\}; \beta = \{1, \ldots, v-1\}$)

$$\begin{aligned}\rho\eta &= \widetilde{\mathscr{S}}(\rho\epsilon, n_\alpha, c^{ij}) = \widehat{\mathscr{S}}(T, n_\alpha, c^{ij}) = \overline{\mathscr{S}}(T, y_\beta, \rho, c^{ij}) \\ &= \acute{\mathscr{S}}(T, y_\beta, C^{ij}).\end{aligned} \tag{9}$$

Four types of dependencies are required for the following purpose: $\widetilde{\mathscr{S}}$ is used for the exploitation of the 2nd law, whereas $\widehat{\mathscr{S}}$, $\overline{\mathscr{S}}$, and $\acute{\mathscr{S}}$ are suitable for the definition of the chemical potentials, μ_α, and the calculation of pressure, p, and the 2nd PIOLA-KIRCHHOFF stresses, $t^{ij} = JF^{im^{-1}}\sigma^{mn}F^{jn^{-1}}$.

From Eq. (7) we obtain by using the product rule

$$\underline{\frac{\partial \widetilde{\mathscr{S}}}{\partial t}} + v^i\underline{\frac{\partial \tilde{\mathscr{S}}}{\partial x^i}} + \widetilde{\mathscr{S}}\frac{\partial v^i}{\partial x^i} + \frac{\partial \phi^i}{\partial x^i} = \zeta. \tag{10}$$

For the underlined terms one can write

$$\frac{\partial \widetilde{\mathscr{S}}}{\partial t} = \frac{\partial \widetilde{\mathscr{S}}}{\partial \rho\epsilon}\underline{\frac{\partial \rho\epsilon}{\partial t}} + \sum_{\alpha=1}^{v}\frac{\partial \widetilde{\mathscr{S}}}{\partial n_\alpha}\underline{\frac{\partial n_\alpha}{\partial t}} + \frac{\partial \widetilde{\mathscr{S}}}{\partial c^{ij}}\frac{\partial c^{ij}}{\partial t}, \tag{11}$$

$$\frac{\partial \widetilde{\mathscr{S}}}{\partial x^i} = \frac{\partial \widetilde{\mathscr{S}}}{\partial \rho\epsilon}\frac{\partial \rho\epsilon}{\partial x^i} + \sum_{\alpha=1}^{v}\frac{\partial \widetilde{\mathscr{S}}}{\partial n_\alpha}\frac{\partial n_\alpha}{\partial x^i} + \frac{\partial \widetilde{\mathscr{S}}}{\partial c^{kl}}\frac{\partial c^{kl}}{\partial x^i}. \tag{12}$$

Inserting the balances (2,4) into Eq. (11) and the result into Eq. (10) yields after rearrangement

$$\zeta = \frac{\partial}{\partial x^i}\left(\phi^i - \frac{q^i}{T} - \sum_{\alpha=1}^{v} j^i_\alpha \frac{\partial \widetilde{\mathscr{S}}}{\partial n_\alpha}\right) + \underbrace{\sum\nolimits_{\alpha=1}^{v} j^i_\alpha \frac{\partial}{\partial x^i}\left(\frac{\partial \widetilde{\mathscr{S}}}{\partial n_\alpha}\right) + q^i \frac{\partial 1/T}{\partial x^i}}_{\mathsf{Q}}$$
$$+ \frac{\partial v^i}{\partial x^j}\left[\frac{\sigma^{ij}_{\mathrm{el}}}{T} + + J^{-2/3}(F^{jk}F^{il} + F^{jl}F^{ik})\frac{\partial \widetilde{\mathscr{S}}}{\partial c^{kl}}\right.$$
$$\left. + \delta^{ij}\left(\widetilde{\mathscr{S}} - \frac{\rho\epsilon}{T} - \sum_{\alpha=1}^{v} n_\alpha \frac{\partial \widetilde{\mathscr{S}}}{\partial n_\alpha} - \frac{2}{3}J^{-2/3}C^{kl}\frac{\partial \widetilde{\mathscr{S}}}{\partial c^{kl}}\right)\right] \geqslant 0. \tag{13}$$

In this context the relation $\dot{c}^{kl} = -\frac{2}{3}J^{-2/3}C^{kl}\nabla^i v^i + J^{-2/3}(F^{jk}F^{il} + F^{ik}F^{jl})\nabla^i v^j$ is used. Furthermore the arrangement of Eq. (13) is based on a certain a priori knowledge of the from of ζ, according to Statement 4 of Section 2.2. Thus we arrange the expression Q to be of the type $\sum F_z D_z$ and extract terms linear in $\nabla^j v^i$ related to the arbitrary terms in Table 1. Now we define the entropy flux ϕ^i as

$$\phi^i = \frac{q^i}{T} + \sum_{\alpha=1}^{v} j^i_\alpha \frac{\partial \widetilde{\mathscr{S}}}{\partial n_\alpha}. \tag{14}$$

Consequently the first row of Eq. (13) vanishes and the remaining equation has the form

$$\mathsf{P}\cdot(\nabla^j v^i) + \mathsf{Q} = \zeta \geqslant 0 \quad \forall(\nabla^j v^i), \tag{15}$$

in which P stands for the long-winding term within the brackets. Here the non-negativity of the entropy production strictly implies $\mathsf{P} = 0$ and $\mathsf{Q} \geq 0$, *i.e.*,

$$\zeta = q^i \frac{\partial 1/T}{\partial x^i} + \sum_{\alpha=1}^{v} j^i_\alpha \frac{\partial}{\partial x^i}\left(\frac{\partial \widetilde{\mathscr{S}}}{\partial n_\alpha}\right). \tag{16}$$

3.2. Classical results

We start by introducing the following representations for the HELMHOLTZ free energy $\rho\varphi$:

$$\rho\varphi = \tilde{\mathscr{F}}(\rho\epsilon, n_\alpha, c^{ij}) = \widehat{\mathscr{F}}(T, n_\alpha, c^{ij}) = \overline{\mathscr{F}}(T, y_\beta, \rho, c^{ij})$$
$$= \acute{\mathscr{F}}(T, y_\beta, C^{ij}). \tag{17}$$

The definition of the *chemical potential* $\mu_\alpha = \partial\widehat{\mathscr{F}}/\partial n_\alpha$ and a *Legendre transfrom* yields $\partial\widetilde{\mathscr{S}}/\partial n_\alpha = -(\partial\widehat{\mathscr{F}}/\partial n_\alpha)/T = -\mu_\alpha/T$. Now j^i_α and q^i in Eq. (16) are chosen such that a quadratic form results, which guarantees non-negativity of the entropy production ζ. Using the constraint of Eq. $(5)_3$, $\sum_\alpha j^i_\alpha = 0$, yields (without coupling terms):

$$j^i_\beta = \sum_{\delta=1}^{v-1} M^{ij}_{\beta\delta}\nabla^j\left[\frac{1}{T}\left(\frac{m_\delta}{m_v}\mu_v - \mu_\delta\right)\right], \tag{18}$$

$$q^i = \kappa^{ij}\nabla^j(1/T) \quad \text{(Fourier's law)}, \tag{19}$$

where $M^{ij}_{\alpha\beta}$ and κ^{ij} are the coefficients of mobility and conductivity.

The relation $\mathsf{P} = 0$ can be exploited in order to find the constitutive equations for p and t^{ij}. Due to limited space we will only present the results, *viz.*

$$p = \rho^2\frac{\partial\bar{\varphi}}{\partial\rho} \quad \text{and} \quad t^{ij} = 2J\rho\frac{\partial\acute{\varphi}}{\partial C^{ij}}. \tag{20}$$

Finally the GIBBS–DUHEM equation, $p + \rho\varphi = \sum_{\alpha=1}^{v} n_\alpha\mu_\alpha$, follows from $p = -\sigma^{kk}_{\mathrm{el}}/3$ and $\mathsf{P} = 0$.

4. Multi-phase mixtures

4.1. Entropy production

For multiphase mixtures one has to take the phase boundaries into account, which can be done by extending the functional representations in Eqs. (9,17) as follows ($\alpha = 1,\ldots,v \wedge \beta = 1,\ldots,v-1$):

$$\rho\eta = \widetilde{\mathbb{S}}(\rho\epsilon, n_\alpha, \nabla^i n_\alpha, \nabla^{ij} n_\alpha, c^{ij}) = \widehat{\mathbb{S}}(T, n_\alpha, \nabla^i n_\alpha, \nabla^{ij} n_\alpha, c^{ij})$$
$$= \overline{\mathbb{S}}(T, y_\beta, \nabla^i y_\beta, \nabla^{ij} y_\beta, \nabla^i\rho, \nabla^{ij}\rho, \rho, c^{ij})$$
$$= \acute{\mathbb{S}}(T, y_\beta, \nabla^i y_\beta, \nabla^{ij} y_\beta, \nabla^i\rho, \nabla^{ij}\rho, C^{ij}) \tag{21}$$

and accordingly

$$\rho\varphi = \widetilde{\mathbb{F}}(\ldots) = \widehat{\mathbb{F}}(\ldots) = \overline{\mathbb{F}}(\ldots) = \acute{\mathbb{F}}(\ldots), \tag{22}$$

where the so-called higher gradients (HGs), $\nabla^i\Xi$ and $\nabla^{ij}\Xi$ with $\Xi = \{n_\alpha, y_\beta, \rho\}$ characterize the spatial gradients of the composition. According to Section 3, the different functions of $\rho\eta$ and $\rho\varphi$ are used for the definition of the chemical potential and the calculation of the mechanical constituitve quantities.

Now the underlined terms of the dissipation inequality in Eq. (10) are re-written as follows:

$$\frac{\partial\widetilde{\mathbb{S}}}{\partial t} = \frac{\partial\widetilde{\mathbb{S}}}{\partial\rho\epsilon}\frac{\partial\rho\epsilon}{\underline{\partial t}} + \frac{\partial\widetilde{\mathbb{S}}}{\partial c^{ij}}\frac{\partial c^{ij}}{\partial t}$$
$$+ \sum_\alpha^v\left(\frac{\partial\widetilde{\mathbb{S}}}{\partial n_\alpha}\frac{\partial n_\alpha}{\underline{\partial t}} + + \frac{\partial\widetilde{\mathbb{S}}}{\partial\nabla^i n_\alpha}\frac{\partial\nabla^i n_\alpha}{\underline{\underline{\partial t}}} + \frac{\partial\widetilde{\mathbb{S}}}{\partial\nabla^{ij} n_\alpha}\frac{\partial\nabla^{ij} n_\alpha}{\underline{\underline{\partial t}}}\right), \tag{23}$$

$$\frac{\partial\widetilde{\mathbb{S}}}{\partial x^k} = \frac{\partial\widetilde{\mathbb{S}}}{\partial\rho\epsilon}\frac{\partial\rho\epsilon}{\partial x^k} + \frac{\partial\widetilde{\mathbb{S}}}{\partial c^{ij}}\frac{\partial c^{ij}}{\partial x^k}$$
$$+ \sum_\alpha^v\left(\frac{\partial\widetilde{\mathbb{S}}}{\partial n_\alpha}\frac{\partial n_\alpha}{\partial x^k} + + \frac{\partial\widetilde{\mathbb{S}}}{\partial\nabla^i n_\alpha}\frac{\partial\nabla^i n_\alpha}{\partial x^k} + \frac{\partial\widetilde{\mathbb{S}}}{\partial\nabla^{ij} n_\alpha}\frac{\partial\nabla^{ij} n_\alpha}{\partial x^k}\right). \tag{24}$$

The underlined terms are treated in the same manner as in Section 3. The double underlined terms must be replaced by the differentiated partial particle balance in Eq. (2), *i.e.*, $\nabla^i(\partial_t n_\alpha)$ and $\nabla^{ij}(\partial_t n_\alpha)$.

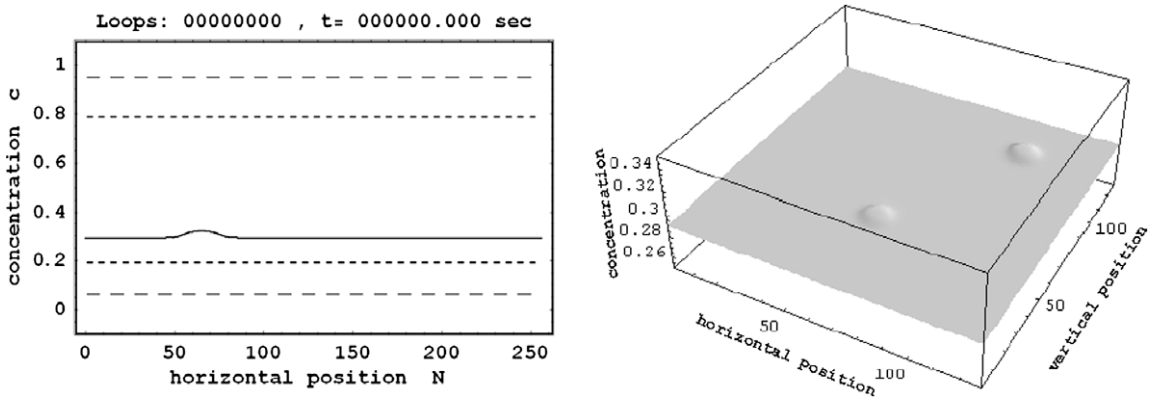

Fig. 1. Initial concentration profiles used for the 1D (one fluctuation) and 2D (two fluctuations) simulations.

Note that Eq. (23) directly indicates which balances and which *differentiated* balances are required during the exploitation of the 2nd law. This fact remedies the aforementioned shortcoming of Liu's procedure, *cf.*, Section 2.2.

By inserting Eqs. (23) and (24) into Eq. (10), and by using the EULER–LAGRANGE derivative

$$\frac{\delta\Diamond}{\delta n_\alpha} = \frac{\partial\Diamond}{\partial n_\alpha} - \nabla^i \cdot \frac{\partial\Diamond}{\partial \nabla^i n_\alpha} + \nabla^{ij} \cdot \frac{\partial\Diamond}{\partial \nabla^{ij} n_\alpha} \tag{25}$$

as well as the relation

$$\dot{n}_\alpha \overset{(\mathrm{def})}{=} \frac{\partial n_\alpha}{\partial t} + v^i \frac{\partial n_\alpha}{\partial x^i} \overset{(2)}{=} -n_\alpha \frac{\partial v^i}{\partial x^i} - \frac{\partial j^i_\alpha}{\partial x^i}, \tag{26}$$

we obtain after a lenghty but straightforward calculation

$$\begin{aligned}
\zeta = \frac{\partial}{\partial x^i}\Bigg\{ & \phi^i - \frac{q^i}{T} - \sum_\alpha^\nu j^i_\alpha \frac{\delta\widetilde{\mathbb{S}}}{\delta n_\alpha} + \sum_\alpha^\nu \dot{n}_\alpha \left[\frac{\partial\widetilde{\mathbb{S}}}{\partial \nabla_i n_\alpha} - \frac{\partial}{\partial x^l}\left(\frac{\partial\widetilde{\mathbb{S}}}{\partial \nabla_{li} n_\alpha} \right) \right] \\
& + \sum_\alpha^\nu \frac{\partial \dot{n}_\alpha}{\partial x^l} \frac{\partial\widetilde{\mathbb{S}}}{\partial \nabla_{li} n_\alpha} - \sum_\alpha^\nu \frac{\partial v^l}{\partial x^k} \frac{\partial n_\alpha}{\partial x^l} \frac{\partial\widetilde{\mathbb{S}}}{\partial \nabla_{ki} n_\alpha} \Bigg\} + q^i \frac{\partial 1/T}{\partial x^i} \\
& + \sum_\alpha^\nu j^i_\alpha \frac{\partial}{\partial x^i}\left(\frac{\delta\widetilde{\mathbb{S}}}{\delta n_\alpha} \right) + \frac{\partial v^i}{\partial x^j} \left\{ \frac{\sigma^{ij}_{\mathrm{el}}}{T} + J^{-2/3}\left(F^{jk}F^{il} + F^{ik}F^{jl}\right) \frac{\partial\widetilde{\mathbb{S}}}{\partial c^{kl}} \right. \\
& - \sum_\alpha^\nu \frac{\partial n_\alpha}{\partial x^i} \left[\frac{\partial\widetilde{\mathbb{S}}}{\partial \nabla_j n_\alpha} - \frac{\partial}{\partial x^l}\left(\frac{\partial\widetilde{\mathbb{S}}}{\partial \nabla_{jl} n_\alpha} \right) \right] - \sum_\alpha^\nu \frac{\partial^2 n_\alpha}{\partial x^i \partial x^l} \frac{\partial\widetilde{\mathbb{S}}}{\partial \nabla_{jl} n_\alpha} \\
& \left. - \delta^{ij}\left[\frac{\rho\epsilon}{T} - \widetilde{\mathbb{S}} + \sum_\alpha^\nu n_\alpha \frac{\delta\widetilde{\mathbb{S}}}{\delta n_\alpha} + \frac{2}{3} J^{-2/3} C^{kl} \frac{\partial\widetilde{\mathbb{S}}}{\partial c^{kl}} \right] \right\} \geqslant 0.
\end{aligned} \tag{27}$$

We define the entropy flux such that the divergence terms of the first three rows vanish, *viz.*

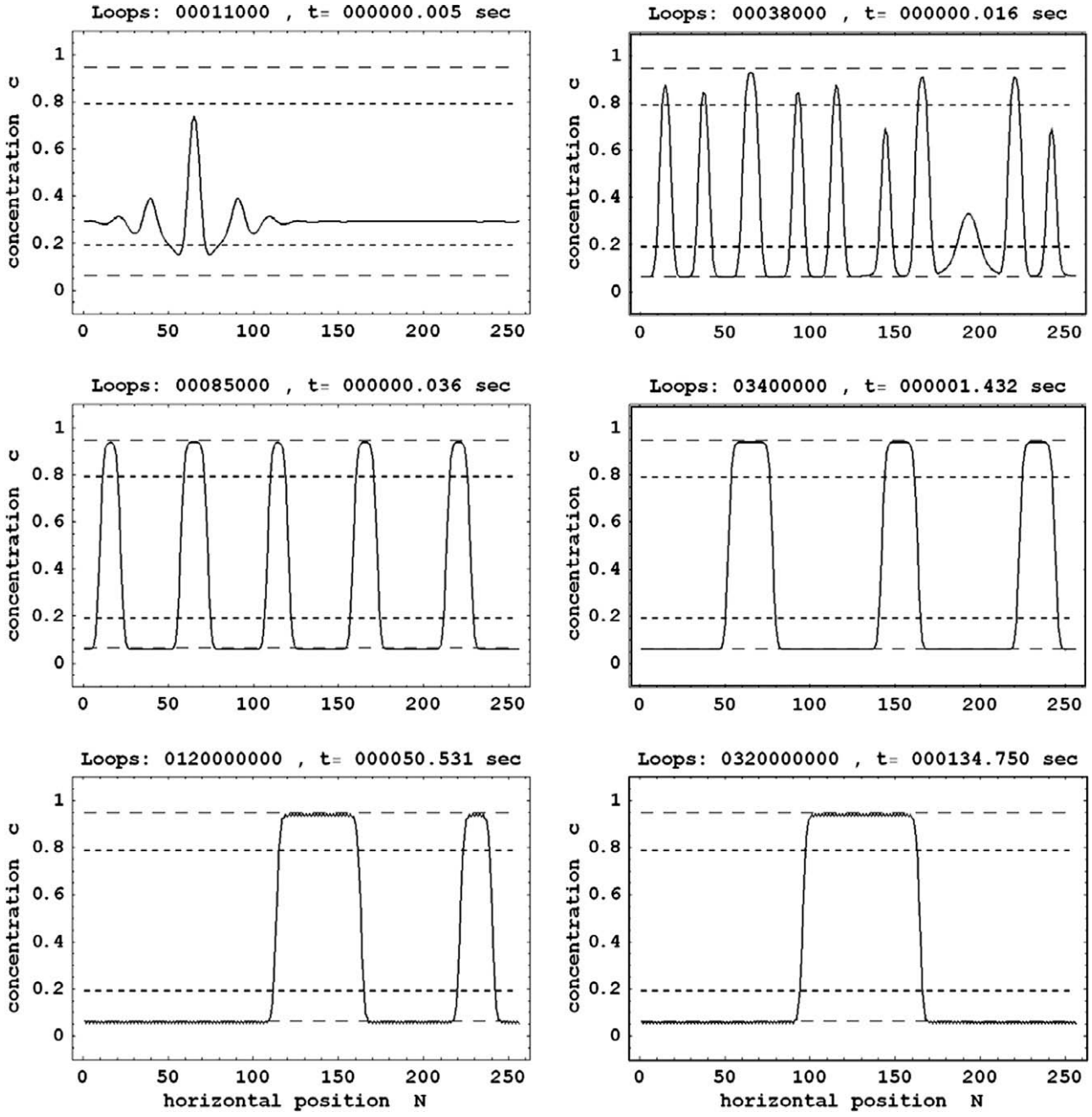

Fig. 2. 1D simulations for a pressure load of $\sigma_0 = -5000$ MPa.

$$\phi^i = \frac{q^i}{T} + \cdots + \sum_{\alpha}^{\nu} \frac{\partial v^l}{\partial x^k} \frac{\partial n_\alpha}{\partial x^l} \frac{\partial \widetilde{\mathbb{S}}}{\partial \nabla_{ki} n_\alpha}. \tag{28}$$

By means of the same arguments as in Section 3 the term within the curly brackets $\{\cdots\}$ of the last four rows vanishes since $\nabla^j v^i \{\cdots\} = 0, \forall (\nabla^j v^i)$. Consequently one finds for the entropy production

$$q^i \frac{\partial 1/T}{\partial x^i} + \sum_{\alpha}^{\nu} j^i_\alpha \frac{\partial}{\partial x^i} \left(\frac{\delta \widetilde{\mathbb{S}}}{\delta n_\alpha} \right) = \zeta \geqslant 0. \tag{29}$$

4.2. Diffusion flux

Eq. (27) can be exploited to find the constitutive relations for, *e.g.*, the pressure, p, the 2nd PIOLA KIRCHHOFF tensor, t^{ij}, and the diffusion flux, j^i_α or J^i_α. However, due to lack of space we will only examine the diffusion flux. To this end we consider Eq. (29). Analogously to the arguments used for the derivation of Eq. (18) we obtain:

$$j^i_\beta = \sum_{\delta=1}^{\nu-1} M^{ij}_{\beta\delta} \nabla^j \left[\frac{1}{T} \left(\frac{m_\delta}{m_\nu} \mu_\nu - \mu_\delta \right) \right], \tag{30}$$

$$J^i_\beta = \sum_{\delta=1}^{\nu-1} B^{ij}_{\beta\delta} \nabla^j \left[\frac{1}{T} \left(\mu^*_\nu - \mu^*_\delta \right) \right] \tag{31}$$

with the definitions of the chemical potential

$$\mu_\alpha \overset{\text{(def)}}{=} \frac{\delta \widehat{\mathbb{F}}}{\delta n_\alpha} \quad \text{or} \quad \mu^*_\alpha \overset{\text{(def)}}{=} \frac{\delta \widehat{\widehat{\mathbb{F}}}}{\delta \rho_\alpha} = \frac{1}{m_\alpha} \frac{\delta \widehat{\mathbb{F}}}{\delta n_\alpha}. \tag{32}$$

Here we introduced the alternative functional representations $\rho\varphi = \widehat{\mathbb{F}}(T, \rho_\alpha, \nabla^i \rho_\alpha, \nabla^{ij} \rho_\alpha, c^{ij}) = \overline{\overline{\mathbb{F}}}(T, c_\beta, \nabla^i c_\beta, \nabla^{ij} c_\beta, \nabla^i \rho, \nabla^{ij} \rho, \rho, c^{ij})$, where c_β denotes the mass concentration.

In some cases it might be pratical to express $\mu^*_\nu - \mu^*_\delta$ in terms of $\delta \overline{\overline{\mathbb{F}}} / \delta c_\delta$. By means of the LEGENDRE transformation the following relation is found:

$$\mu^*_\nu - \mu^*_\delta = \sum_{\lambda=1}^{\nu-1} \frac{\delta \overline{\overline{\mathbb{F}}}}{\delta c_\lambda} \left(\frac{\delta_{\nu\lambda}}{\rho} - \frac{\delta_{\delta\lambda}}{\rho} \right) = -\frac{1}{\rho} \frac{\delta \overline{\overline{\mathbb{F}}}}{\delta c_\delta}. \tag{33}$$

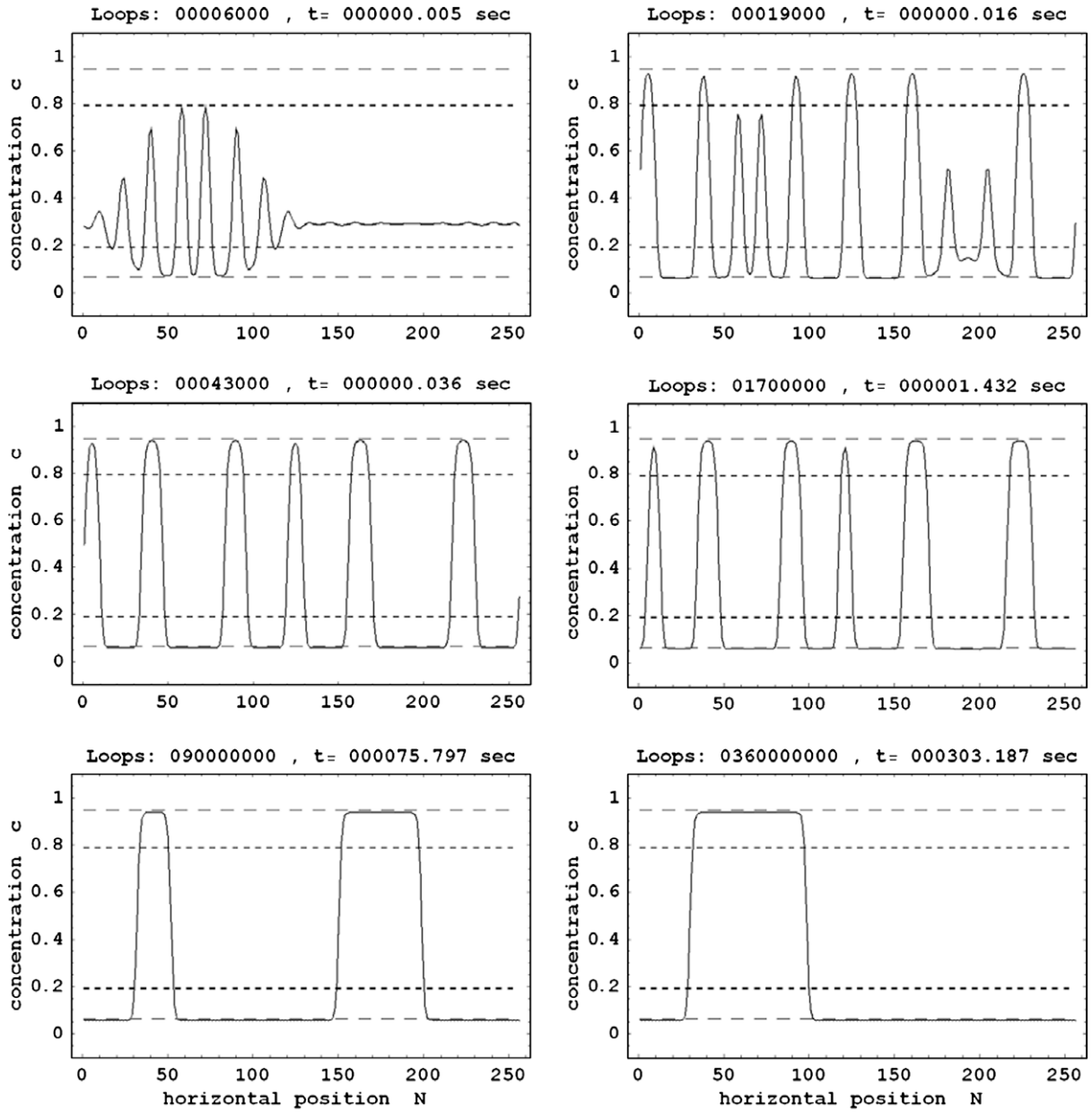

Fig. 3. 1D simulations for a tensile load of $\sigma_0 = +5000$ MPa.

4.3. Binary alloys and extended diffusion equation

Next we investigate the binary case, namely a solid mixture A–B, in which the following relations hold:

$$\rho = \rho_A + \rho_B \quad \text{and} \quad c_B = 1 - c_A. \tag{34}$$

In order to predict the phase evolution characterized by the (smoothly changing) concentration field $c = c_B$ within the mixture we reformulate the partial mass balance in Eq. (1) as follows ($T = \text{const}$, $J^i = J^i_B$ and $\overline{B}^{ij}(T) = B^{ij}_{AA}/T$):

$$\rho \frac{dc}{dt} = -\frac{\partial J^i}{\partial x^i}, \quad J^i \overset{(33)}{=} -\overline{B}^{ij}(T)\nabla^j\left(\frac{1}{\rho}\frac{\delta \overline{\overline{\mathbb{F}}}}{\delta c}\right). \tag{35}$$

At this point the question arises, how $\overline{\overline{\mathbb{F}}}$ depends on the higher derivatives $\nabla^i c$ and $\nabla^{ij} c$. For this reason we follow the strategy of Cahn and Hilliard [4], and expand $\overline{\overline{\mathbb{F}}}$ into a TAYLOR series around the (homogeneous) reference state (no gradients):

$$\overline{\overline{\mathbb{F}}} = \overline{\overline{\mathbb{F}}}_0(T, c, \varepsilon^{ij}) + l^k(c, \varepsilon^{ij})\nabla^k c - a^{kl}(c, \varepsilon^{ij})\nabla^{kl} c + \frac{1}{2} b^{kl}(c, \varepsilon^{ij})\nabla^k c \nabla^l c + \cdots \tag{36}$$

with the so-called Higher Gradient Coefficients (HGCs) $l^k = \partial \overline{\overline{\mathbb{F}}}/\partial \nabla^k c$, $a^{kl} = \partial \overline{\overline{\mathbb{F}}}/\partial \nabla^{kl} c$, and $b^{kl} = \partial^2 \overline{\overline{\mathbb{F}}}/(\partial \nabla^k c \partial \nabla^l c)$, which can be *exactly* calculated by means of atomistic theories [2]. In particular it follows that due to the periodic arrangement of the lattice $l^k = 0$ holds. Furthermore the HELMHOLTZ free energy density of the homogeneous state consists of a pure thermodynamical part and a thermo-elastic part, *viz.* $\overline{\overline{\mathbb{F}}}_0 = \overline{\overline{\mathbb{F}}}_{th} + \overline{\overline{\mathbb{F}}}_{el}$, where $\overline{\overline{\mathbb{F}}}_{th}$ can be determined from experimental phase equilibrium data. For $\overline{\overline{\mathbb{F}}}_{el}$ we simply assume HOOKE's law:

$$2\overline{\overline{\mathbb{F}}}_{el} \approx (\varepsilon^{ij} - \alpha^{ij}\Delta T) C^{ijkl}(T, c)(\varepsilon^{kl} - \alpha^{kl}\Delta T), \tag{37}$$

where α^{ij} stand for the coefficients of thermal expansion.

Note that in [1,5] an equivalent version of Eq. (35) is used. Here the authors chose a LAGRANGEian description which can be derived from Eq. (35) by simply performing the replacement: $x^i \to X^i$ and $\rho \to \rho_0$, where ρ_0 denotes the *constant* mass density of the homogeneous reference state. Inserting Eq. (36) into Eq. (35) the following **Extended Diffusion Equation** (EDE) is finally obtained ($A_{kl} := \partial a_{kl}/\partial c + b_{kl}$)

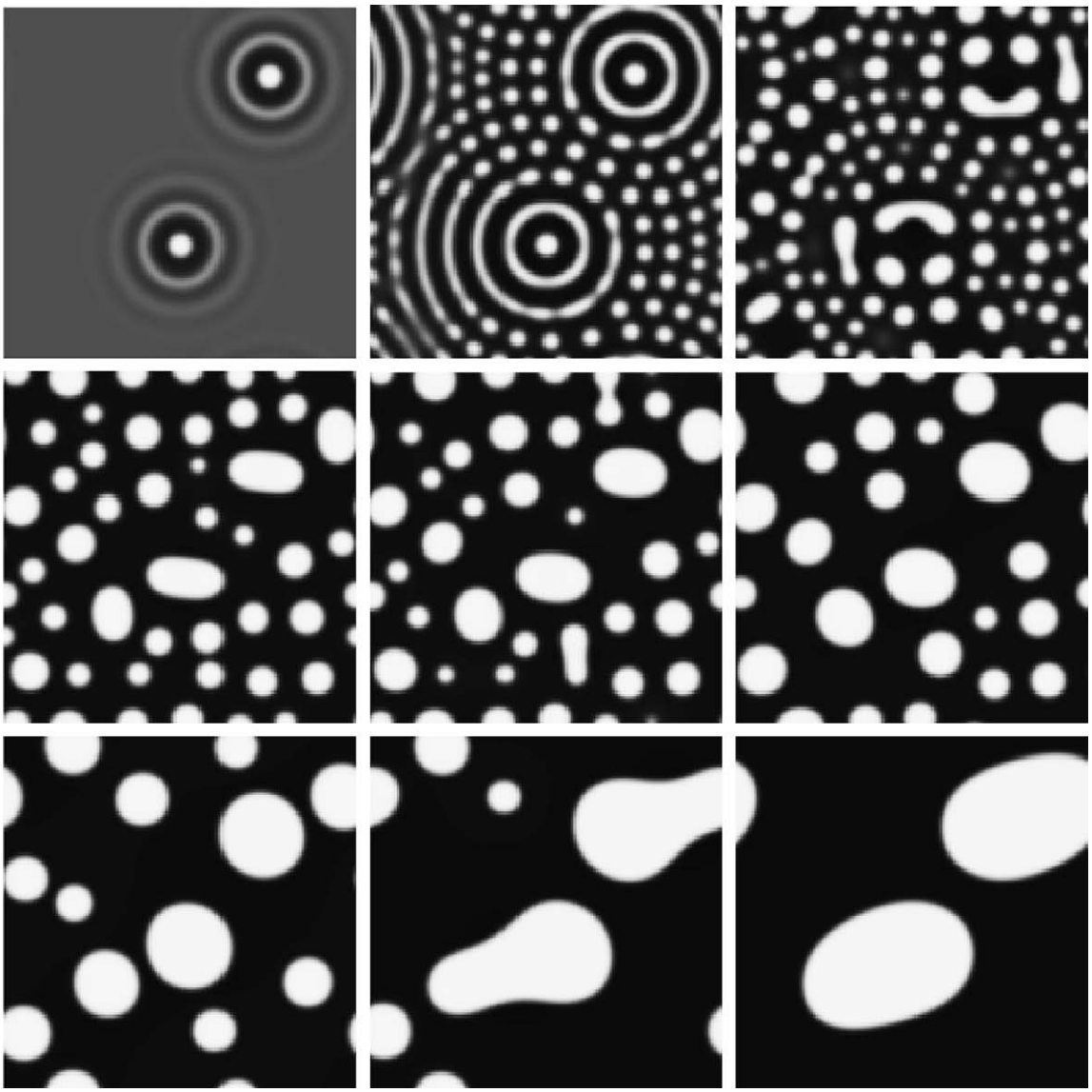

Fig. 4. 2D simulations by means of an explicit EULER method: after 5.8×10^{-3}, 1.17×10^{-2}, 2.2×10^{-2}, 5.1×10^{-2}, 6.6×10^{-2}, 9.5×10^{-2}, 0.4, 0.87, and 1.3 s.

$$\rho_0 \frac{\mathrm{d}c}{\mathrm{d}t} = \rho_0 \frac{\partial}{\partial X^i}\left[M^{ij}\frac{\partial}{\partial X^j}\left(\frac{\partial[\mathbb{F}_{\mathrm{th}}+\mathbb{F}_{\mathrm{el}}]}{\partial c} - 2A^{kl}\frac{\partial^2 c}{\partial X^k \partial X^l} - \frac{\partial A^{kl}}{\partial c}\frac{\partial c}{\partial X^k}\frac{\partial c}{\partial X^l} - 2\frac{\partial A^{kl}}{\partial \varepsilon^{mn}}\frac{\partial c}{\partial X^k}\frac{\partial \varepsilon^{mn}}{\partial X^l} - \frac{\partial^2 a^{kl}}{\partial \varepsilon^{op}\partial \varepsilon^{mn}}\frac{\partial \varepsilon^{op}}{\partial X^k}\frac{\partial \varepsilon^{mn}}{\partial X^l} - \frac{\partial a^{kl}}{\partial \varepsilon^{mn}}\frac{\partial^2 \varepsilon^{mn}}{\partial X^k \partial X^l}\right)\right] \quad (38)$$

in which we redefine the mobility by $M^{ij} \overset{(\mathrm{def})}{=} \rho_0^2 \overline{B}^{ij}$.

Eq. (38) can be interpreted as a generalization of the well-established Cahn–Hilliard equation and represents a nonlinear PDE of fourth order, which must be solved numerically in order to investigate the temporal change of the concentration field $c(X^i, t)$.

5. Numerical studies

5.1. Material data and computational realization

In what follows we turn the attention to the binary alloy Ag–Cu at 1000 Kelvin and put: $\mathrm{A} \equiv \mathrm{Ag}, \mathrm{B} \equiv \mathrm{Cu}, c \equiv c_{\mathrm{B}} = c_{\mathrm{Cu}}$. Moreover we restrict our simulations to the following *two* cases:

(1) One-dimensional simulations under the presence of so-called *line strains*, *i.e.*:

$$\varepsilon^{ij} \doteq \varepsilon^{11} = \varepsilon(x,t) \wedge \varepsilon^{ij} \doteq 0 \ \forall i,j = \{1,2\}. \quad (39)$$

Following the strategy in [1] the set of required material data reduces to ($T = \mathrm{const} := 1000$ K): $\mathbb{F}_{\mathrm{th}}(c)$, $C^{11}_{\alpha,\beta}$, $M_{\alpha,\beta}$, $a(\varepsilon, c)$, $b(\varepsilon, c)$, and $A(\varepsilon, c)$.

(2) Two-dimensional simulations for the *strain-free case*. Then the last three terms in the diffusion flux of the EDE vanish. Furthermore the *absence* of local thermo-mechanical strains, $\varepsilon^{ij} = 0$, reduces the mobility and the HGCs to the following isotropic form ($i,j = \{1,2\}$), [2]:

$$\Xi^{ij} = \Xi\delta^{ij}, \quad \Xi = \{M_{\alpha,\beta}, a(c), b(c), A(c)\}. \quad (40)$$

Hence the required set of material data is given by: $\mathbb{F}_{\mathrm{th}}(c)$, $M(c)$, $a(c)$, $b(c)$, and $A(c)$.

$\mathbb{F}_{\mathrm{th}}(T,c)$ is fitted according to the MARGULES-ansatz by using discrete phase equilibrium data, available from MTdata™, [1]. The HGCs are exactly calculated as functions of ε^{ij} and c by means of

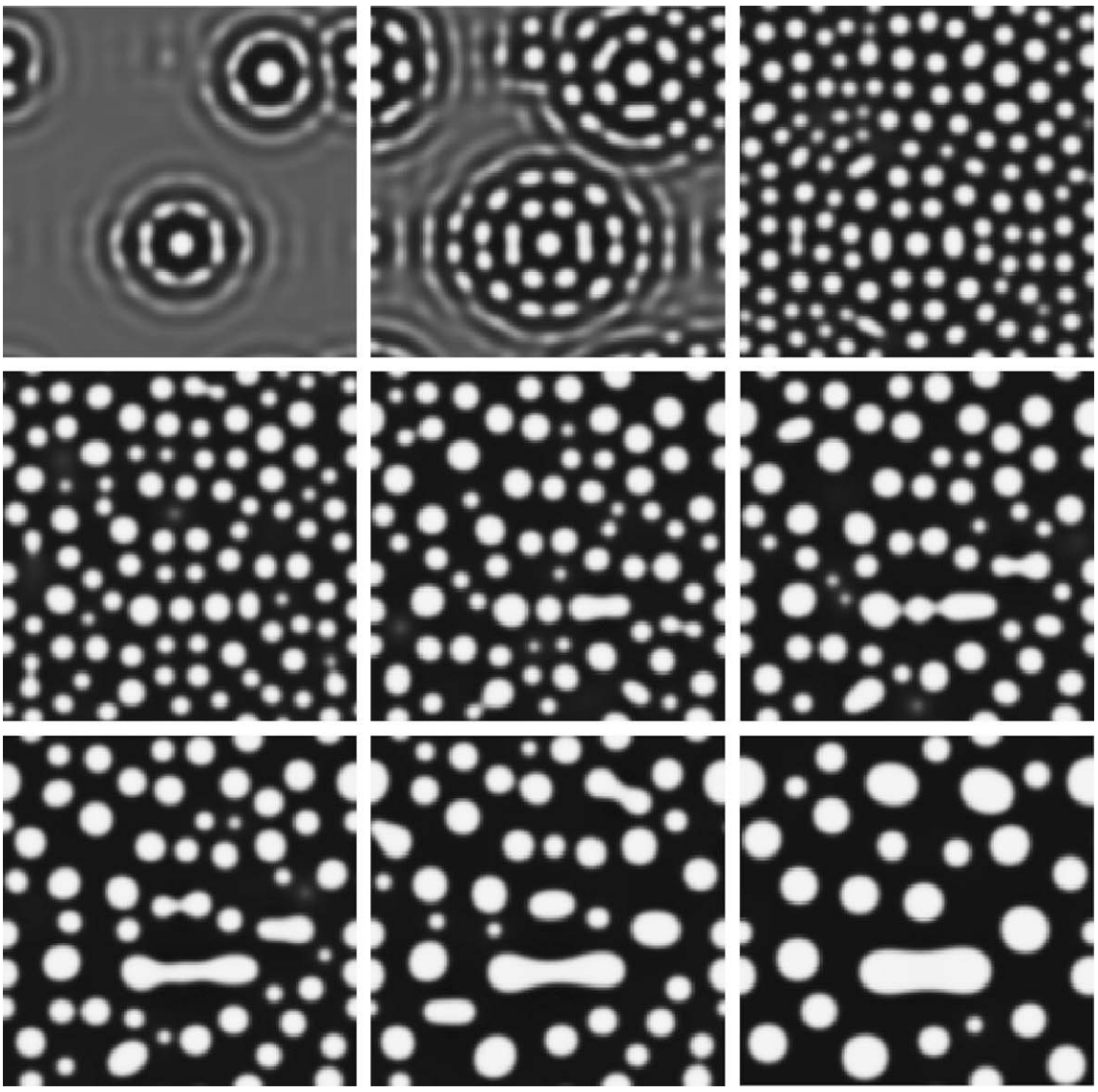

Fig. 5. 2D simulations by means of the time-adaptive implicit RUNGE-KUTTA method provided by the RADAU routine: after 6.3×10^{-3}, 8.13×10^{-3}, 1.0×10^{-2}, 1.8×10^{-2}, 2.5×10^{-2}, 2.9×10^{-2}, 3.3×10^{-2}, 4.5×10^{-2}, and 8.2×10^{-2} s.

the Embedded-Atom-Method (EAM), [1,2], and range between 1 and 8×10^{-10}N. The remaining data are taken from the literature or databases, *e.g.*, [10].

In order to solve the EDE numerically we used a FORTRAN 90 code. In particular the spatial derivatives were discretized by finite differences and replaced by an algebraic expression in FOURIER space, [1]. The required discrete FOURIER transforms were performed by means of the FFTPack5 package, [11]. For the time integration we applied an explicit EULER method and - for comparison – an implicit, time adaptive RUNGE–KUTTA method using the free available RADAU package, [8].

Furthermore we used a spatial discretiziation of $N = 256$ (1D) and $N \times N = 128 \times 128$ (2D) grid points. The area of the investigated RVE was $L = 0.6 \cdot 10^{-7}$ m (1D) and $L = 0.5 \cdot 10^{-7}$ m (2D). Finally, the (constant) time integration steps applied during the EULER method were $\mathrm{d}t = 0.2 \cdot 10^{-6}$ s (1D, pressure loading), $\mathrm{d}t = 0.4 \cdot 10^{-6}$ s (1D, tensile loading), and $\mathrm{d}t = 1 \cdot 10^{-6}$ s (2D, EULER), [3].

5.2. Phase separation and coarsening in Ag–Cu

We start with an undercooled (unstable) one-phase *eutectic* mixture ($c^{\mathrm{eut}}_{\mathrm{AgCu}} = 0.29$) characterized by the (slightly pertubed) homogeneous concentration profile as illustrated in Fig. 1. Here the outermost dashed lines denote the equilibrium concentrations ($c_\alpha = 0.063$, $c_\beta = 0.945$) of the decomposed two-phase mixture and the innermost dashed lines are the spinodal concentrations ($c_{\mathrm{sp},1} = 0.19$, $c_{\mathrm{sp},2} = 0.79$), which enclose the unstable region.

According to the unstable state the binary Ag–Cu alloy immediately begins to decompose and subsequently proceeds with coarsening. Unusually high loading was applied during the 1D simulations in Figs. 2 and 3 in order to observe their impact within manageable computational times. Furthermore it seems that pressure loadings increase the coarsening rate in comparison to tensile loadings[1]. Finally we emphasize that the implicit time integration by means of the RADAU routine is extremely time consuming which cannot be compensated by larger (adaptive) time steps. Therefore the simulated time period in Fig. 5 is much smaller than the according one in Fig. 4, [3].

6. Summary and future prospects

In order to investigate the micromorphological development in solid mixtures a theory was presented, which allows to construct the required constitutive equations consistently with the 2nd law. First, we have shown the agreement of the obtained results with those of classical thermodynamics (single phase mixtures), and, second, we extend the theory to multicomponent and multiphase materials and derive a general form for the diffusion flux containing so-called higher gradients to model the smoothly changing phase boundaries. Moreover, we have shown how thermo-elastic fields change the free energy and, consequently, enter the diffusion equation. After that we specified to binary alloys and presented various numerical studies in 1D and 2D for the brazing solder Ag–Cu.

Summarizing the preceding sections the following three items stand for the main focus of the article:

- A revisited entropy principle in combination with an alternative exploitation of the 2nd law (*cf.*, *e.g.*, [7] for comparison) was introduced to model diffusion-controlled phase transformations in (elastically) deformable, solid mixtures.
- An extended diffusion equation was derived, which incorporates classical Fickian ("downhill") diffusion, surface tension effects (represented by the HGC-terms), and local elastic strains due to external loadings and misfits. In particular, the consideration of strain-depending HGCs in Eq. (36) represents an extension of the classical Cahn–Hilliard/Cahn–Larché equation.
- Numerical simulations were performed based on exactly calculated HGCs following from an atomistic theory, [2]. These values are considerably smaller than typical values from literature, *e.g.*, [12], and lead to a pretty sharp phase boundary (*cf.*, [1] for a more detailed discussion of the numerical consequences).

Furthermore it is worth mentioning that the presented numerical simulations are performed on extremely small length scales ($L \simeq 600$ Å). Typical diameters of SMT[2] solder balls are much bigger, *viz.* $d \approx 150$—350 μm. However, due to the used *equidistant* spatial discretization a sufficiently large number of grid points, N, accompanied by a small RVE length, L, is required to model the "sharp" phase boundaries realistically within manageable computational times. In order to investigate the aforementioned SMT length scales recently developed numerical methods based on adaptive spatial discretizations seem to be very promising for future work, [13].

Acknowledgements

Close cooperation with the WIAS BERLIN (Dr. W. Dreyer) and assistance of A. BRANDMAIR during the numerical implementation is grateful acknowledged. Furthermore this work is supported by the DEUTSCHE BUNDESSTIFTUNG UMWELT (DBU).

References

[1] T. Böhme, W.H. Müller, Comput. Mater. Sci. 43 (1) (2007) 221–228.
[2] T. Böhme, W. Dreyer, W.H. Müller, Continuum Mech. Therm. 18 (7–8) (2007) 411–441.
[3] A. Brandmair, Anwendung höherer Gradiententheorien zur Simulation des Entmischungs-und Vergröberungs-prozesses in bleifreien Lotwerkstoffen, Diploma Thesis, Institut für Mechanik, TU Berlin, 2007.
[4] J.W. Cahn, J.E. Hilliard, J. Chem. Phys. 28 (1958) 258–267.
[5] W. Dreyer, W.H. Müller, Int. J. Solids Struct. 37 (2000) 3841–3871.
[6] C. Făciu, A. Molinari, J. Phys. IV 6 (1996). C1-45–C1-54.
[7] M.E. Gurtin, Physica D 92 (1996) 178–192.
[8] E. Hairer, G. Wanner, Universite de Geneve, Department de Mathematiques, CH-1211 Geneve, Switzerland. <www.unige.ch/hairer/prog/stiff/radau.f>.
[9] I.-S. Liu, Arch. Rat. Mech. Anal. 46 (1972) 131–148.
[10] E.A. Brandes, G.B. Brook, Smithells Metals Reference Book, seventh ed., Reed Educational and Professional Publishing Ltd., 1992.
[11] P. Swarztrauber, R. Valent, University Corporation for Atmospheric Research, 2004, Download under: <www.cisl.ucar.edu/css/software/fftpack5/>.
[12] R.L.J.M. Ubachs, P.J.G. Schreurs, M.G.D. Geers, J. Mech. Phys. Solids 52 (2004) 1763–1792.
[13] U. Weikard, Numerische Lösung der Cahn-Hilliard-Gleichung und der Cahn-Larché-Gleichung, Ph.D. thesis, Institut für Angewandte Mathematik, Universität Bonn, Germany, 2002.

[1] We also performed 1D simulations *without* external loadings. The results are not presented here due to a lack of space, but note, that compressive *as well as* tensile loadings accelerate the coarsening rate w.r.t. the stress-free simulations.

[2] **S**urface **M**ount **T**echnology.